A simple and effective model for Jones matrix to evaluate the transmission performance of Savart polariscope*

Wu Hai-Ying(吴海英)[a], Zhang Chun-Min(张淳民)[a]†, and Li Jie(李 杰)[b]

[a] *Non-equilibium Condensed Matter and Quantum Engineering Laboratory, the Key Laboratory of the Ministry of Education, School of Science, Xi'an Jiaotong University, Xi'an* 710049, *China*

[b] *School of Electronic and Information Engineering, Xi'an Jiaotong University, Xi'an* 710049, *China*

(Received 9 September 2009; revised manuscript received 19 May 2010)

Starting from the wave normal tracing treatment in the Savart polariscope that relates the Jones matrix to its transmission performance, this paper establishes a simple and effective model for the Jones matrix at an arbitrary incidence in the spatial domain. Analytical expressions of all the matrix components are determined with the consideration of all the main impact factors. This model needs only a few parameters hence it is convenient to be employed to evaluate the propagation performance of any birefringent optical system. The simulated results obtained with it demonstrate that this model gives a precise representation of the characteristic of light propagation in the Savart polariscope. This would provide useful suggestions for the design, calibration, and performance improvement of any other birefringent polarisation element and optical system.

Keywords: wave normal tracing method, Jones matrix, transmission performance, Savart polariscope

PACC: 4215D, 0760F, 4225L

1. Introduction

With the development of polarisation optics, a considerable number of various birefringent elements or polarisation optical systems are becoming more and more popular in many applications, such as filters as appropriate tunable elements inside or outside laser cavities,[1,2] retarders for phase modulation,[3] wave-plates in the observation of polarisation status[4] and birefringent prisms to introduce linearly complete polarised light.[4,5] They are also necessary components in stationary polarisation interferometers,[6] polarisation imaging spectrometers[7,8] and spectropolarimeters.[9,10]

The birefringence phenomenon in these polarisation elements often introduces unique performance in light transmission which is obviously different from that in the isotropic components. A simple and useful theoretical means for predicting the overall transmission property of birefringent polarisation elements is the evaluation of the Jones matrix. Consequently, exploiting the analytical relationship between the transmission performance and the Jones matrix is mandatory. Referring to the existing literatures, we find that several Jones matrices have been developed for several cases. The matrix for a filter tilted at Brewster' angle was deduced by Bloom *et al.* for the special case in which the optical axis is parallel to the plate surface.[11,12] Later, Shidong and Jurgen *et al.* extended this representation into a more general case where the optical axis is at an arbitrary angle to the plate surface.[13,14] Recently, considering the splitting effect between the two waves, Yang *et al.* proposed an improved Jones matrix for a birefringent plate with the optical axis parallel to the surface.[15,16]

However, the Jones matrices mentioned above all concern a birefringent plate or filter for some special cases including the optical axis on the plate surface, the plane of incidence is perpendicular to the plate surfaces, or the incident angle is fixed at the Brewster angle. Besides, some important factors having influence on the transmission performance were not taken into account. In the present research, starting from wave normal tracing treatment that relates the

*Project supported by the State Key Program of National Natural Science Foundation of China (Grant No. 40537031), the National Natural Science Foundation of China (Grant No. 40875013), the National Defense Basic Scientific Research Project, China (Grant No. A1420080187), the National High Technology Research and Development Program of China (Grant No. 2006AA12Z152).

†Corresponding author. E-mail: zcm@mail.xjtu.edu.cn

© 2010 Chinese Physical Society and IOP Publishing Ltd

Jones matrix to the transmission performance, the authors attempt to determine the explicit Jones matrix of the Savart polariscope for which the two combined crystal plates have orthogonal principlal sections. The corresponding transmission performance of Savart polariscope is detailedly depicted in company with all the important impact factors including the incident angle, the azimuthal angle of incidence, the orientations of the two optical axes, and the dispersion effect due to the varying wavelengths of incident light. This model proves to be simple with only a few parameters and finds an effective application in the evaluation of transmission performance for the systems combining birefringent component with arbitrary incident orientation and arbitrary optical axis direction.

To the best of our knowledge, this paper presents a deterministic and complete means to characterize the transmission properties of the Savart polariscope and this has never been done before in literatures. All the work we finished would provide theoretical suggestions for the performance improvement of any other birefringent network.

The outline of this paper is as follows. First, the beam-splitting principle of the Savart polariscope as well as the wave normal tracks of light in the Savart plates are both detailedly presented in Section 2. Then in Section 3 the Jones transformation matrix is deduced and the exact formulae expressions of all the matrix elements are directly derived. Considering all the important impact factors, the transmission behaviour of the Savart polariscope is particularly discussed in this section. Finally we give conclusions of the work we have finished in this paper and indicate the point for the future research.

2. Operation principle and wave normal tracing in the Savart polariscope

The operation principle of the Savart polariscope has been described in detail in many previous papers.[17−26] Here we only provide a brief description about it. Savart polariscope is a birefringent laterally shearing beam splitter which is made of uniaxial crystal material. As illustrated in Fig. 1, the Savart polariscope is made up of two identical plates cut at 45° to the optical axis of system and having their principal sections perpendicular to each other. When a beam of light incidents on the polariscope with a normal angle, it will be split into two linearly polarised components including one parallel and the other perpendicular to the optic axis.

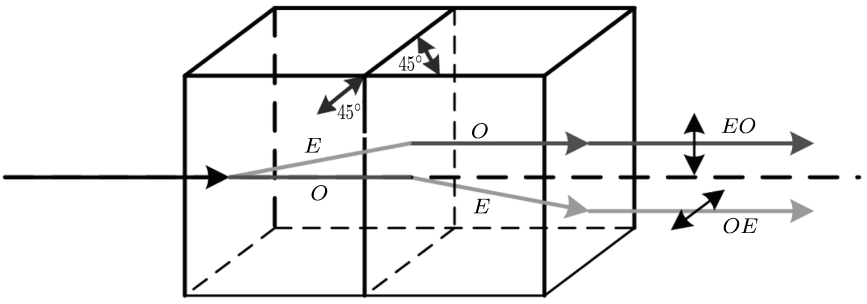


Fig. 1. Schematic diagram of the Savart polariscope.

The light beam that incidents on the left plate of the Savart polariscope, is resolved into two polarisation components, the ordinary component O with its polarisation orientation perpendicular to its principal plane and the extraordinary component E parallel to its principal plane. Holding on their vibration directions, the two components are respectively changed into the extraordinary ray E and the ordinary ray O in the right plate due to the mutually orthogonal principal sections. The two output beams both transmit along the orientation of incident light.

Employing the wave normal tracing method, we describe the propagation of light in Savart polariscope as illustrated in Fig. 2. Here the coordinates are chosen such that the $x-z$ plane lies in the plane of the page with the y-axis pointing into the paper. The x-axis represents the normal direction of the plate surface to the right level direction and the z-axis orients at the vertical direction (i.e. , $\boldsymbol{y} = \boldsymbol{z} \times \boldsymbol{x}$).

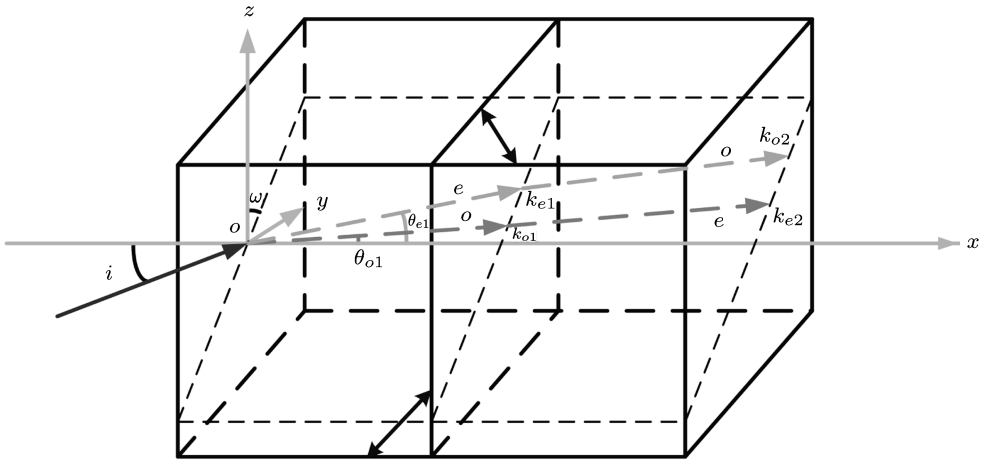


Fig. 2. Wave normal tracing in the Savart polariscope.

Suppose that a beam of light incidents on the left plate at an angle i with the incidence plane oriented at an arbitrary angle with respect to the principal section of the left plate. The incident plane contains the incident light and the normal to the input interface. Note that the surrounding medium is considered to be vacuum here. According to the Snell's law, the refractive angles θ_{o1} and θ_{e1} in the left plate, for the ordinary and extraordinary wave normal respectively, can be given by

$$\sin i = n_o \sin\theta_{o1}, \tag{1}$$

$$\sin i = n_1 \sin\theta_{e1}, \tag{2}$$

where n_o and n_1 represent the refractive indices of the ordinary and extraordinary wave, respectively. Here n_1 can be expressed as

$$n_1 = \frac{1}{\sqrt{\left(\dfrac{1}{n_o^2} - \dfrac{1}{n_e^2}\right) \times \cos^2\gamma_1 + \dfrac{1}{n_e^2}}}, \tag{3}$$

where γ_1 denotes the angle between the optical axis and the propagation direction of the extraordinary wave vector inside the left plate. Another parameter α_1, which is the angle between the incidence plane and the plane defined by the optic axis and the refractive ray of the extraordinary wave, should be introduced to the wave normal tracing process. They can be expressed by the following relationships:[14]

$$\cos\gamma_1 = \sin\theta_{e1}\cos\varepsilon\cos\omega + \sin\varepsilon\cos\theta_{e1}, \tag{4}$$

$$\cos\alpha_1 = \frac{\cos\theta_{e1}\cos\varepsilon\cos\omega - \sin\varepsilon\sin\theta_{e1}}{\sqrt{1-\cos^2\gamma_1}}. \tag{5}$$

Here ε is the angle formed by the optic axis and the plate plane and it values 45° for the Savart polariscope, while ω represents the angle between the incidence plane and projection of the optic axis onto the surface of the left plate. Substituting Eqs. (2) and (4) into Eq. (3), we can derive exact formulation of n_1 as a function of i and ω in the following form:

$$n_1(i,\omega) = \sqrt{\frac{-b_1(i,\omega) + \sqrt{b_1^2(i,\omega) - 4\times a_1(i,\omega)\times c_1(i,\omega)}}{2\times a_1}} \tag{6}$$

with

$$a_1 = \frac{1}{4}\times\left(\frac{1}{n_o^2}+\frac{1}{n_e^2}\right)^2,$$

$$b_1(i,\omega) = -\left(\Delta_1(i,\omega)\times\left(\frac{1}{n_o^2}+\frac{1}{n_e^2}\right) + \left(\frac{1}{n_o^2}-\frac{1}{n_e^2}\right)^2\times\sin^2 i\times\cos^2\omega\right),$$

$$c_1(i,\omega) = \Delta_1^2(i,\omega) + \left(\frac{1}{n_o^2}-\frac{1}{n_e^2}\right)^2\times\sin^4 i\times\cos^2\omega,$$

and

$$\Delta_1(i,\omega) = 1 - \frac{1}{2} \times \left(\frac{1}{n_o^2} - \frac{1}{n_e^2}\right) \times \sin^2 i \times \cos^2 \omega + \frac{1}{2} \times \left(\frac{1}{n_o^2} - \frac{1}{n_e^2}\right) \times \sin^2 i.$$

According to the definitions above, the wave normal functions of the ordinary wave o and the extraordinary wave e in the left plate of the Savart polariscope can be respectively formulated by

$$\frac{x}{\cos\theta_{o1}} = \frac{y}{\sin\omega\sin\theta_{o1}} = \frac{z}{\cos\omega\sin\theta_{o1}}, \tag{7}$$

and

$$\frac{x}{\cos\theta_{e1}} = \frac{y}{\sin\omega\sin\theta_{e1}} = \frac{z}{\cos\omega\sin\theta_{e1}}. \tag{8}$$

Then the locations of the o-wave $\hat{k}_{o1}$ and e-wave $\hat{k}_{e1}$ intersected on the interface between the two Savart plates can be determined by

$$\begin{cases} x_{o1} = d, \\ y_{o1} = d\sin\omega\tan\theta_{o1}, \\ z_{o1} = d\cos\omega\tan\theta_{o1}, \end{cases}$$

$$\begin{cases} x_{e1} = d, \\ y_{e1} = d\sin\omega\tan\theta_{e1}, \\ z_{e1} = d\cos\omega\tan\theta_{e1}. \end{cases} \tag{9}$$

Similarly, all the parameters introduced by the right plate in the Savart polariscope can be calculated from Eqs. (1)–(9) by replacing ω by $\omega + \pi/2$. The location coordinates of the two waves $\hat{k}_{e2}$ and $\hat{k}_{o2}$ on the exit interface can be given by

$$\begin{cases} x_{e2} = d, \\ y_{e2} = d\sin\left(\omega + \dfrac{\pi}{2}\right)\tan\theta_{e2}, \\ z_{e2} = d\cos\left(\omega + \dfrac{\pi}{2}\right)\tan\theta_{e2}, \end{cases}$$

$$\begin{cases} x_{o2} = d, \\ y_{o2} = d\sin\left(\omega + \dfrac{\pi}{2}\right)\tan\theta_{o2}, \\ z_{o2} = d\cos\left(\omega + \dfrac{\pi}{2}\right)\tan\theta_{o2}, \end{cases} \tag{10}$$

where θ_{e2} is the angle formed by the o-wave direction in the left plate and the interface normal orientation of the right plate. Likewise, θ_{o2} represents the angle between the e-wave direction in the left plate and the interface normal orientation of the right plate. They can be formulated by θ_{o1} and θ_{e1} in the left plate.

Combining with the geometrical optical method, the detailed phase retardations produced by o-wave and e-wave in the left and right plates can be obtained as

$$\delta_{ol} = \frac{2\pi}{\lambda}\left(n_o\sqrt{x_{o1}^2 + y_{o1}^2 + z_{o1}^2} + \sqrt{(x_{e1} - x_{o1})^2 + (y_{e1} - y_{o1})^2 + (z_{e1} - z_{o1})^2}\sin i\right), \tag{11}$$

$$\delta_{el} = \frac{2\pi}{\lambda}\left(n_1\sqrt{x_{e1}^2 + y_{e1}^2 + z_{e1}^2}\right), \tag{12}$$

$$\delta_{er} = \frac{2\pi}{\lambda}\left(n_2\sqrt{x_{e2}^2 + y_{e2}^2 + z_{e2}^2}\right), \tag{13}$$

$$\delta_{or} = \frac{2\pi}{\lambda}\left(n_o\sqrt{x_{o2}^2 + y_{o2}^2 + z_{o2}^2} + \sqrt{(x_{e2} - x_{o2})^2 + (y_{e2} - y_{o2})^2 + (z_{e2} - z_{o2})^2}\sin i\right). \tag{14}$$

3. Jones matrix and transmission performance of Savart polariscope

Based on the wave normal tracing method in the Savart polariscope, its Jones transmission matrix will be established in this section. It is well known that the Jones matrix has a useful application in the evaluation of the transmission characteristics of optical systems which comprise birefringent elements. The explicit expression of the Jones transformation matrix for a birefringent plate can be expressed by

$$\boldsymbol{M} = \begin{pmatrix} \exp(\mathrm{i}\,\delta_e)\cos^2\alpha + \exp(\mathrm{i}\,\delta_o)\sin^2\alpha & (\exp(\mathrm{i}\,\delta_e) - \exp(\mathrm{i}\,\delta_o))\sin\alpha\cos\alpha \\ (\exp(\mathrm{i}\,\delta_e) - \exp(\mathrm{i}\,\delta_o))\sin\alpha\cos\alpha & \exp(\mathrm{i}\,\delta_o)\cos^2\alpha + \exp(\mathrm{i}\,\delta_e)\sin^2\alpha \end{pmatrix}. \tag{15}$$

Thus we can obtain the Jones matrix for the two Savart plates as

$$J_{\text{left}} = \begin{pmatrix} L_{11} & L_{12} \\ L_{21} & L_{22} \end{pmatrix}$$

$$= \begin{pmatrix} \exp(\mathrm{i}\,\delta_{e1})\cos^2(\alpha_1) + \exp(\mathrm{i}\,\delta_{o1})\sin^2(\alpha_1) & (\exp(\mathrm{i}\,\delta_{e1}) - \exp(\mathrm{i}\,\delta_{o1}))\sin(\alpha_1)\cos(\alpha_1) \\ (\exp(\mathrm{i}\,\delta_{e1}) - \exp(\mathrm{i}\,\delta_{o1}))\sin(\alpha_1)\cos(\alpha_1) & \exp(\mathrm{i}\,\delta_{o1})\cos^2(\alpha_1) + \exp(\mathrm{i}\,\delta_{e1})\sin^2(\alpha_1) \end{pmatrix}, \quad (16)$$

$$\boldsymbol{J}_{\mathrm{right}} = \begin{pmatrix} R_{11} & R_{12} \\ R_{21} & R_{22} \end{pmatrix}$$

$$= \begin{pmatrix} \exp(\mathrm{i}\,\delta_{e2})\cos^2(\alpha_2) + \exp(\mathrm{i}\,\delta_{o2})\sin^2(\alpha_2) & (\exp(\mathrm{i}\,\delta_{e2}) - \exp(\mathrm{i}\,\delta_{o2}))\sin(\alpha_2)\cos(\alpha_2) \\ (\exp(\mathrm{i}\,\delta_{e2}) - \exp(\mathrm{i}\,\delta_{o2}))\sin(\alpha_2)\cos(\alpha_2) & \exp(\mathrm{i}\,\delta_{o2})\cos^2(\alpha_2) + \exp(\mathrm{i}\,\delta_{e2})\sin^2(\alpha_2) \end{pmatrix}. \quad (17)$$

Substituting all the corresponding parameters into Eqs. (16) and (17), all the four complex elements for the two Jones matrixes $\boldsymbol{J}_{\mathrm{left}}$ and $\boldsymbol{J}_{\mathrm{right}}$ can be directly obtained. Thus the total matrix for the Savart polariscope can be obtained by performing the matrix multiplication in sequence as

$$\boldsymbol{J} = \begin{pmatrix} J_{11} & J_{12} \\ J_{21} & J_{22} \end{pmatrix}$$

$$= J_{\mathrm{right}} J_{\mathrm{left}} = \begin{pmatrix} R_{11} & R_{12} \\ R_{21} & R_{22} \end{pmatrix} \begin{pmatrix} L_{11} & L_{12} \\ L_{21} & L_{22} \end{pmatrix}$$

$$= \begin{pmatrix} R_{11}L_{11} + R_{12}L_{21} & R_{11}L_{12} + R_{12}L_{22} \\ R_{21}L_{11} + R_{22}L_{21} & R_{21}L_{12} + R_{22}L_{22} \end{pmatrix}. \quad (18)$$

In the following section, the corresponding transmission property of the Savart polariscope will be simulated and analysed in detail. According to the Jones matrix given above, the transmission properties can be characterized by the following quantities:[16] $T_{\mathrm{pp}} = |J_{11}|^2$, $T_{\mathrm{ps}} = |J_{12}|^2$, $T_{\mathrm{sp}} = |J_{21}|^2$and $T_{\mathrm{ss}} = |J_{22}|^2$.

Referring to the parameters used in the polarisation interference imaging spectrometer which has been demonstrated by ourselves, we chose the integrant components as: the Savart polariscope here is made up of two identical calcite plates with the single plate thickness $d = 15$ mm, and the incident angle of light is limited in the range $0 - 3°$. The transmission variables T_{pp}, T_{ps}, T_{sp} and T_{ss} of the Savart polariscope is detailedly analysed in the following four situations.

(i) If the incident wavelength is fixed at $\lambda = 632.8$ nm, and the corresponding birefringent parameter values are chosen i.e. the refractive index for the extraordinary wave $n_e = 1.48515$ and for the ordinary wave $n_o = 1.65567$, the four transmission quantities varying with the azimuthal angle ω are shown in Fig. 3 where the incident angle i is fixed at a value 3°.

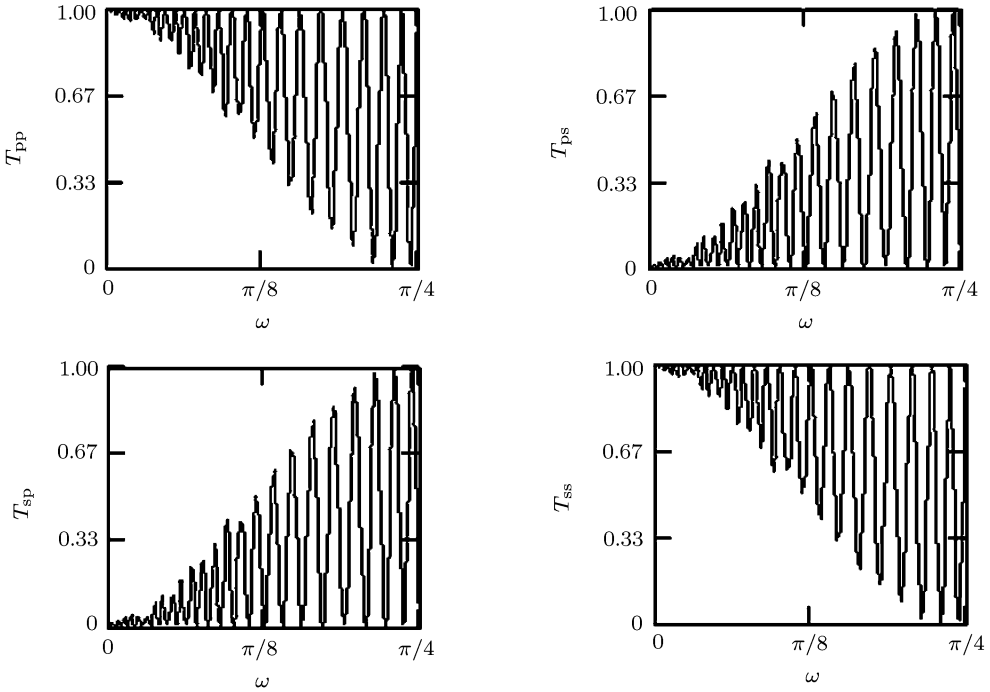


Fig. 3. Transmission characteristics versus the azimuthal angle ω.

It can be seen that the four transmission values all show sharp variations in the same region $0-1$. The two diagonal quantities take on the same silhouette and trend. The variations around $\omega = \pi/4$ reach the maximum.

(ii) Supplied with the same parameters in the first situation above except the azimuthal angle which is fixed at $\omega = 0$, the resultant transmission variation tendencies with the increasing incident angles are presented in Fig. 4. It shows that the variation here is much milder than that produced by varying azimuthal angles. In this case, $T_{\rm pp}$ and $T_{\rm ss}$ vary from 0.985 to 1 whereas $T_{\rm ps}$ and $T_{\rm sp}$ are in the region $0-0.015$. Hence the total transmission is principally contributed by $T_{\rm pp}$ and $T_{\rm ss}$.

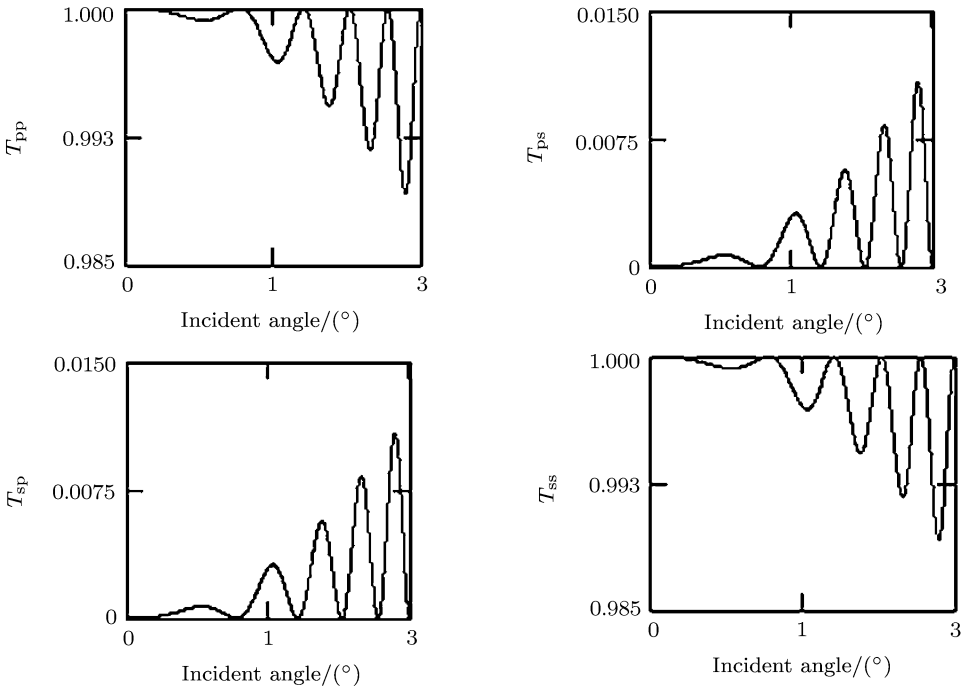


Fig. 4. Transmission characters versus the incident angle i.

(iii) In the third situation, considering that two optical axes of the Savart plates have an identical deviation angle θ from the original 45° orientation and remaining all the parameters determined above, we can obtain the transmission variations with θ as illustrated in Fig. 5.

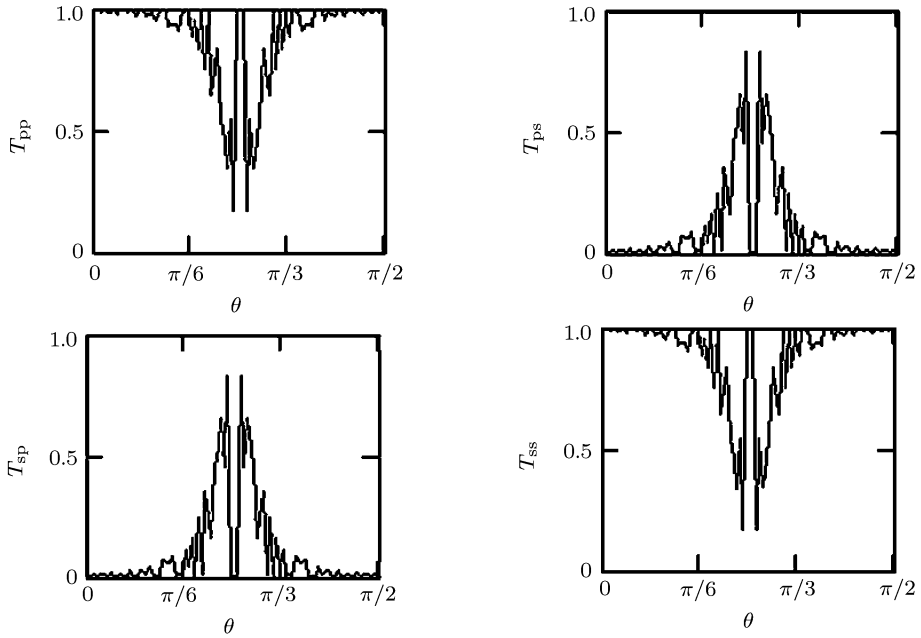


Fig. 5. Transmission characters versus the deviation angle θ of the plate's optical axis from the 45° direction.

It can be seen that when the value of θ is around 45° there are remarkable fluctuations in the transmission curves. In practice, the deviation from the 45° direction of the optical axes of the Savart polariscope should be limited in the range $0 \sim \pi/12$ to make sure that there is no distinct influence on the energy transmission. The case in which the two optical axes have different deviation angles is similar to this situation.

(iv) In the last situation, it is assumed that the refraction indices for the e-wave and o-wave change with the incident wavelength varying from 0.48 μm to 0.96 μm. The refractive index formulae with the wavelength can be presented in the following forms:

$$n_o(\lambda) = \sqrt{2.69705 + \frac{0.0192064}{\lambda^2 - 0.01820} - 0.0151624\lambda^2}, \tag{19}$$

$$n_e(\lambda) = \sqrt{2.18438 + \frac{0.0087309}{\lambda^2 - 0.01018} - 0.0024411\lambda^2}. \tag{20}$$

Substituting the two equations above into the Jones matrix as given by Eq. (16), we can acquire the variation curves of the transmission characters shown in Fig. 6. There are three extremums denoting the maximum and minimum of the energy transmission and this will be carefully considered in the system design for the improvement of optical efficiency.

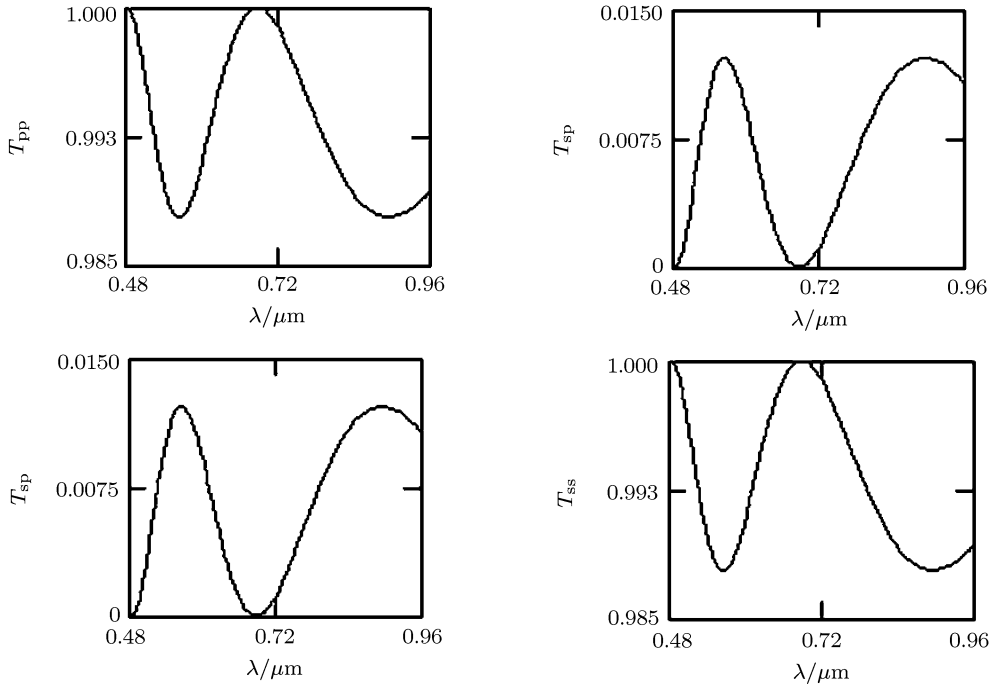


Fig. 6. Transmission characteristics versus incident wavelength λ.

In conclusion, according to Figs. 3–6 we can see that the transmission properties in the Savart polariscope of the polarisation interference imaging spectrometer are closely related to the azimuthal angle ω of incidence, the incident angle i, the optical axis directions of the two Savart plates and the wavelength of incident light. All the impact factors should be taken into account in the design of the whole optical system, such that high energy transmission could be achieved. This is very important for all optical system especially in remote sensing applications.

4. Conclusion

Starting from wave normal tracing in the Savart polariscope, we deduce and analyse a simple and useful model for Jones matrix to evaluate its transmission performance. The tracks of the extraordinary wave and

the ordinary wave in propagation are clearly described. An explicit Jones matrix for the Savart polariscope is derived and exact formulae of all the matrix components are presented. As an example, the transmission property of the Savart polariscope in the polarisation interference imaging spectrometer is discussed in detail. The simulated results indicate that the incident angle, the azimuthal angle of incidence, the incident wavelength and the optical axes of the Savart polariscope are all important factors which would affect the transmission characteristics. And this demonstrates that our model provides an exact representation for the birefringent elements with arbitrary incidence when the optical axes orient at arbitrary orientations in space. The work finished in this paper will provide theoretical and practical suggestions for the study, design, experiment and engineering of the polarisation interference imaging spectrometers as well as other birefringent polarisation networks. It should be noted that all the impact factors including i, ω, λ, and θ will inevitably have influence on the energy transmission, the polarisation distribution and the interference fringe contrast of the whole system, and thus great care should be taken for the performance improvement of the polarisation interference imaging spectrometer. This will be the point in our future work.

References

[1] Zhu S D 1990 *Appl. Opt.* **29** 410
[2] Zhu X, Kean P N and Sibbett W 1989 *Opt. Lett.* **14** 1192
[3] Schirmer J and Schmidt-Kaler T 2000 *Opt.Commun.* **176** 313
[4] Drlscoll W G and Vaughan W 1978 *Handbook of Optics* (Newyork: Mc-Graw-HillBook Co.) p102, p21
[5] Azzam R M A and Bashara N M 1977 *Ellipsometry and Polarized Light* (New York: North-Holland Publishing Co.) p367
[6] Yu H W and Meng S X 1996 *Opt. Eng.* **35** 2310
[7] David W F and Andrew R H 2004 *Opt. Express* **12** 5368
[8] Gao Z, Oka K, Tsuyoshi I and Naoshi B 2002 *Appl. Opt.* **41** 734
[9] Nathan H, Kazuhiko O and Eustace L Dereniak 2007 *Opt. Lett.* **32** 2100
[10] Luo H T, Oka K, Edward D, Kudenov M, James S and Eustace L D 2008 *Appl. Opt.* **47** 4413
[11] Bloom A L 1974 *J. Opt. Soc. Am.* **64** 447
[12] Hodgkinson I J and Vukusic J I 1978 *Appl. Opt.* **17** 1944
[13] Jurgen M, Eberhard S and Thomas M 1992 *Appl. Opt.* **31** 5022
[14] Zhu X N 1994 *Appl. Opt.* **33** 3502
[15] Yang T, Jing H M and Liu D H 2006 *J. Opt.* A: *Pure Appl. Opt.* **8** 295
[16] Yang T, Wan X K, Jing X M and Liu D H 2007 *J. Opt.* A: *Pure Appl. Opt.* **9** 222
[17] Zhang C M, Bin X L and Zhao B C 2000 *Proc. SPIE* **4087** 957
[18] Zhang C M, Bin X L and Zhao B C 2004 *J. Opt.* A: *Pure Appl. Opt.* **6** 815
[19] Wu H Y, Zhang C M and Zhao B C 2008 *Acta Phys. Sin.* **57** 3499 (in Chinese)
[20] Zhang C M, Zhao B C, Bin X L, Li Y C and Peng Z H 2006 *Proc. SPIE* **6150** 615001
[21] Wu H Y, Zhang C M, Zhao B C and Li Y C 2009 *Acta Phys. Sin.* **58** 1642 (in Chinese)
[22] Wu H Y, Zhang C M and Zhao B C 2008 *Acta Phys. Sin.* **58** 930 (in Chinese)
[23] Zhang C M, Zhao B C and Bin X L 2004 *Appl. Opt.* **43** 6090
[24] Mu T K, Zhang C M and Zhao B C 2009 *Opt.Commun.* **282** 1699
[25] Zhang C M, Zhao B C, Yuan Z L and Huang W J 2009 *J. Opt.* A: *Pure Appl. Opt.* **11** 085401
[26] Zhang C M, Ren W Y and Mu T K 2010 *Chin. Phys.* B **19** 024202